Proceedings of the EuroGNC 2013, 2nd CEAS Specialist Conference on
Guidance, Navigation & Control, Delft University of Technology, Delft,
The Netherlands, April 10-12, 2013

Automatic UAV Landing with Ground Target Maintained in the Field of View

Laurent Burlion and Henry de Plinval

Abstract In this paper, a key capability for UAV visual servoing in automatic landing is investigated: the possibility to add an output constraint to a given control law, namely that a ground target point be maintained inside the camera field of view (FoV). This method has been recently developed, and the present study represents an application of this method, which can be applied to any nonlinear system. First, a control law for UAV automatic landing is proposed. Then, the output constraint method is presented. Later, the method is applied to the UAV landing case. Finally, simulation results are presented, which show the relevance of the method. The approach thus solves a key element of any visual servoing problem: the possibility to maintain a given object inside the camera field of view.

1 Introduction

Various studies have recently investigated the possibility to succesfully land a UAV through a vision-based control law. In [1], a linear visual servoing control scheme for the automatic hovering of a blimp is proposed. The same authors have later proposed [2] a visual servoing scheme for vanishing features with application to UAV automatic landing. A nonlinear framework for UAV automatic landing is proposed in In [3]; it is based on 2D information from the camera image and the bi-normalised Plücker coordinates.
These studies make an important assumption for practical implementation: the object of interest is assumed to remain inside the camera field of view along the land-

Laurent Burlion
ONERA - The French Aerospace Lab, 2, avenue Edouard Belin, Toulouse, France, e-mail: laurent.burlion@onera.fr

Henry de Plinval
ONERA - The French Aerospace Lab, 2, avenue Edouard Belin, Toulouse, France, e-mail: henry.de-plinval@onera.fr

ing trajectory. Some other studies have considered ensuring this property instead of making this assumption. Thus, [4] ensures this property through optimal paths computation and homography matrix switches. Also, [5] controls a rigid body while maintaining a target inside the field of view through Backstepping motion. There, smart strategies are proposed to maintain the object of interest inside the videocamera field of view. However, these strategies cannot be directly implemented for automatic UAV landing, since they would lead to infeasible trajectories for such aircraft: a conventional aircraft is not able to rotate at a given spot in space, and its linear / rotational velocities are not independent degrees of freedom.

In this study, we use the so-called homography matrix to maintain a given ground point inside the videocamera field of view. This matrix represents the image transformation corresponding to a change in the camera point of view. It has been exploited n different studies. [6] uses it to reconstruct the 3D structure based on two different views. In [7], a similar approach is proposed in the context of vision based car platooning. [8] builds a complete visual map-less navigation from the use of homographies. The analytical decomposition of the homography matrix has also been investigated in terms of position / orientation, as [9] or [10]. The notion of homography itself has also been extended, as the super-homography in [11]. [12] proposes a framework to control a robot based on information extracted from the homography matrix.

Imposing a constraint on given outputs or inputs is a problem which arises in most of the control applications and have been investigated in the past by many researchers. Note that the input constraint problem is rather less difficult and was more investigated in the past decades (see for instance [13]).

One can divide the proposed solutions to these problems into two groups : in the first group, the methods check if the constraints will be violated by predicting the future while in the second, at each time the methods try to avoid the constraints. Regarding linear systems, future prediction is easier; moreover, dedicated LMI-based methods have been proposed [14, 15]. Finally, state and input constraints problems are close to one another since there exists [16, 17] a relationship between a constrained output and an induced constrained input (whose constraints values are state dependent and so time-varying).

One of the authors of this paper has recently [18] generalized this idea to nonlinear systems and shown how to convert one output constrained nonlinear system into one input constrained nonlinear system. When comparing with existing results [19, 20, 21, 22, 23], [24, 25, 26], this method has several advantages : no prediction is used and/or it does not require the nonlinear system to be in some special form. Note however that this preliminary work only addressed the problem to constrain one output which is not sufficient to solve the applicative problem investigated in this paper.

The structure of this paper is the following: the first section presents the problem at hand. Section 2 proposes our main results: after some theoretical developments, the method is presented, which transforms the FoV constraints into a state-dependent saturation functions applied to the baseline flight control laws. Section 3 illustrates our results on the motivating example of a landing UAV. It also provides some nu-

merical results. Finally we conclude the paper together with future research directions.

1.1 Notations

Let $\mathscr{R}$ (resp. $\mathscr{N}$) denote the set of real numbers (resp. natural integers). In this paper, we are interested in nonlinear systems of dimension $n \in \mathscr{N}$. For $i \in [1,n]$, we note e_i the vector of the Euclidean basis of $\mathscr{R}^n$.

Given $\sigma \in \mathscr{C}^1(\mathscr{R}^n,\mathscr{R})$, $L_f\sigma := \sum_{i=1}^n f_i\partial_i\sigma$ denotes its Lie-derivative with respect to f.

Throughout this paper, we will use the following useful notations :

Given $r \in \mathscr{N}$ real numbers $K_1,\ldots,K_r$, we note

$$K_{j,r} := \prod_{i=j}^{r} K_i$$

and we also pose (for convenience) :

$$\forall j \in \mathscr{N},\ K_{j+1,j} := 1$$

Given two real numbers $z_{\min} < z_{\max}$, we note :

$$z \longmapsto Sat_{z_{\min}}^{z_{\max}}(z) = \max(z_{\min}, \min(z_{\max}, z))$$

the saturation function of a variable between $z_{\min}$ and $z_{\max}$

1.2 Variables list

Here is a list of the variables introduced in the text:

Variable name	Description
g	gravitation constant
$\omega = (p,q,r)$	angular velocity
m	aircraft mass
V	linear velocity
F_{aero}	aerodynamic forces
F_{propu}	propulsion force
x,y,z	cartesian coordinates
ϕ, θ, ψ	roll, pitch, yaw angles
γ	trajectory slope
α	angle of attack
α_0	equilibrium angle of attack
S	wings surface
V_0	linear velocity
ρ	air density
C_{z_α}	aerodynamic coefficient relating angle of attack and lift
H	homography matrix
R, p	rotation matrix and translation vector from reference image pose
d^*, n^*	distance to ground and unit vector normal to the ground
w_i	output to be constrained
$(x_c(t), y_c(t), z_c(t))$	reference trajectory
$(\delta_x, \delta_y, \delta_z) = (x - x_c, y - y_c, z - z_c)$	position error with respect to reference trajectory
$K_i, K_{j,r}$	user defined constant numbers and
	product of these numbers

2 Problem statement

In this section, the considered problem is presented. We are interested in forcing a given function of the system's state to remain inside a desired range. In this article, the case of an unmanned landing aircraft is addressed. This aircraft is supposed to make use of a videocamera for e.g. visual servoing purpose, for instance in order for state estimate improvement purpose. This aircraft is controlled via a feedback such that it remains on a predefined landing trajectory. We aim at showing how such a basic control law can be modified so as to take into account an additional output constraint. In the present case, the constraint consists in maintaining a given ground object in the camera field of view.

2.1 Aircraft model

In this paper we assume that the aircraft attitude remains small -which is mostly the case for an aircraft landing-, so that a linear assumption is made. However, nonlinear terms do appear in the model through the image model. The retained model is that of a standard aircraft, with main aerodynamics effects taken into account. **In order to simplify the computations carried in this paper, we assume direct control of the aircraft through angular velocity vector**

$$\omega := (p,q,r)^T$$

Thus, the propulsion and aerodynamics moments do not need to be computed.
The aircraft acceleration is modeled by :

$$m\dot{V} = F_{aero} + F_{propu} \tag{1}$$

The propulsion force is chosen such that the norm of the speed $\|V\|$ is considered constant all along the landing phase ($\|V\| = V_0$).
With the small angles assumption and some approximations, the **longitudinal dynamics** of the aircraft is given by:

$$\begin{cases} \dot{x} & = V_0 \\ \dot{z} & = -V_0\gamma \\ mV_0\dot{\gamma} & = \frac{1}{2}\rho S V_0^2 C_{z\alpha}(\alpha - \alpha_{eq}^0) \\ \dot{\alpha} & = q - \dot{\gamma} \end{cases} \tag{2}$$

and the **lateral dynamics**:

$$\begin{cases} \dot{y} & = V_0\psi \\ \dot{\psi} & = -\frac{g}{V_0}\varphi \\ \dot{\varphi} & = p \end{cases} \tag{3}$$

We also assume that $\beta = 0$ and $r = \frac{g\varphi}{V_0}$.
Coefficients are as follows:

$$\begin{cases} S & = 260m^2 \\ m & = 1,1.10^5 kg \\ C_{z\alpha} & = 5 \\ \alpha_{eq}^0 & = 3.7185deg \\ V_0 & = 70m.s^{-1} \\ g & = 9.81m.s^{-2} \\ \rho & = 1.225kg.m^{-3} \end{cases} \tag{4}$$

2.2 Image modeling, homography matrix

In the studied application case, a UAV uses a videocamera for e.g. state estimation improvement. Thus, given features on the ground have to be maintained inside the videocamera field of view. This constraint is computed based on the UAV state. To do this, we use the so-called homography matrix. This matrix has been used in the past in visual servoing applications ([6], [7], [8]). We assume that a set of "reference" pictures of the landing runway taken along the desired landing trajectory are available. In this article, we consider one reference image, available for comparison with the current image seen by the videocamera. At each instant, we aim at maintaining one particular object described by a pointing direction in the reference image inside the field of view. This can then be exploited to maintain the runway in the field of view. The homography matrix can be computed based on a comparison between the current and reference images (see [27, 12] for more details and associated computation algorithms). This matrix represents the transformation between the target's points coordinates from the reference pose to the current pose. It is given by:

$$H = R^T - \frac{1}{d^*} R^T p n^{*T} \tag{5}$$

where R, p, are the rotation matrix and translation vector from the current to the reference frame, d^* the distance from the UAV reference position (where the picture was taken) to the ground plane and n^* the normal to the target plane, expressed in the reference frame. Based on this matrix, the current image coordinates of a ground object described by a pointing direction in the reference frame can be computed. To do this, we first compute Hv^*, with v^* being this pointing direction. This vector $v = Hv^*$ is normalized (projection onto the image plane) through $w = (v_2/v_1; v_3/v_1)$. The obtained vector w contains the 2D coordinates of the point of interest in the current image. Consequently, in order to maintain this point in the field of view, one needs to enforce the following inequalities:

$$-1 \leq w_1 \leq 1$$

and

$$-1 \leq w_2 \leq 1$$

Note that ensuring instead $-0.5 \leq w_2 \leq 0$ would constrain the object to stay inside a given sector of the current image. Now, these constraints will be considered in the application case.

The derivative of the homography matrix is needed for computations. It is computed as:

$$\dot{H} = -S(\omega)H - \frac{1}{d^*} \bar{v} n^{*T}$$

with $\bar{v}, \omega$ being the linear and angular velocities. The image coordinate points could be computed directly, without this step of computing the homography matrix;

however, this choice has been made in order to insist on its relationship with recent works on this topic.

2.3 First control design

The following trajectory was retained for the landing phase:

$$x_c(t) = x(t)\ ;\ y_c(t) = 0\ ;\ z_c(t) = x(t)tan(\gamma_c)$$

where $\gamma_c = -3deg$.
Let: $\delta_y = y - y_c$,$\delta_z = z - z_c$,$\delta_\alpha = \alpha - \alpha_{eq}^0$ and $\delta\gamma = \gamma - \gamma_c$.
The basic control laws are defined with the following form:

$$\begin{cases} q = k_z\delta_z + k_\gamma\delta_\gamma + k_\alpha\delta_\alpha \\ p = k_y\delta_y + k_\chi\chi + k_\phi\phi \end{cases} \tag{6}$$

Its coefficients are computed through classical backstepping design with a time scale separation assumption. (Note that the system to control being linear, other design as LQ or poles placement can have been used).
Fig. 1 represents the result obtained when starting with an initial error on z and y and applying the proposed control law with no FoV constraint so far:

2.4 Output constraint method

The proposed output constraint method [18] is based on the key remark that an output constraint can be recast into an input saturation. The principle is recalled in the annex, while Fig.2 is a representation of the relative degree 2 case.

To use this method for the landing problem with FoV constraint, let us first provide an extension of the first theorem presented in ([18]). It consists in extending the result to several outputs and inputs.

Theorem 1 Consider a nonlinear system in the class (8) with full state measurement (i.e $y = x$) and z and u belonging to $\mathscr{R}^2$. Let $z_{1,\min} < z_{1,\max}$ and $z_{2,\min} < z_{2,\max}$ be four real numbers. Let $z = [z_1, z_2]^T$, $u = [u_1, u_2]^T$, $g = [g_1\ g_2]$ and $\sigma(x) = [\sigma_1(x), \sigma_2(x)]$. Assume z_1 (resp. z_2) is of relative degree $r_1 \in \mathscr{N}_{>0}$ (resp. r_2) and that the following 2×2 matrix $M_z(x)$ is invertible for all $x \in \mathscr{R}^n$

$$M_z(x) := \begin{bmatrix} L_{g_1}L_f^{r_1-1}\sigma_1(x)\ L_{g_2}L_f^{r_1-1}\sigma_1(x) \\ L_{g_1}L_f^{r_2-1}\sigma_2(x)\ L_{g_2}L_f^{r_2-1}\sigma_2(x) \end{bmatrix}$$

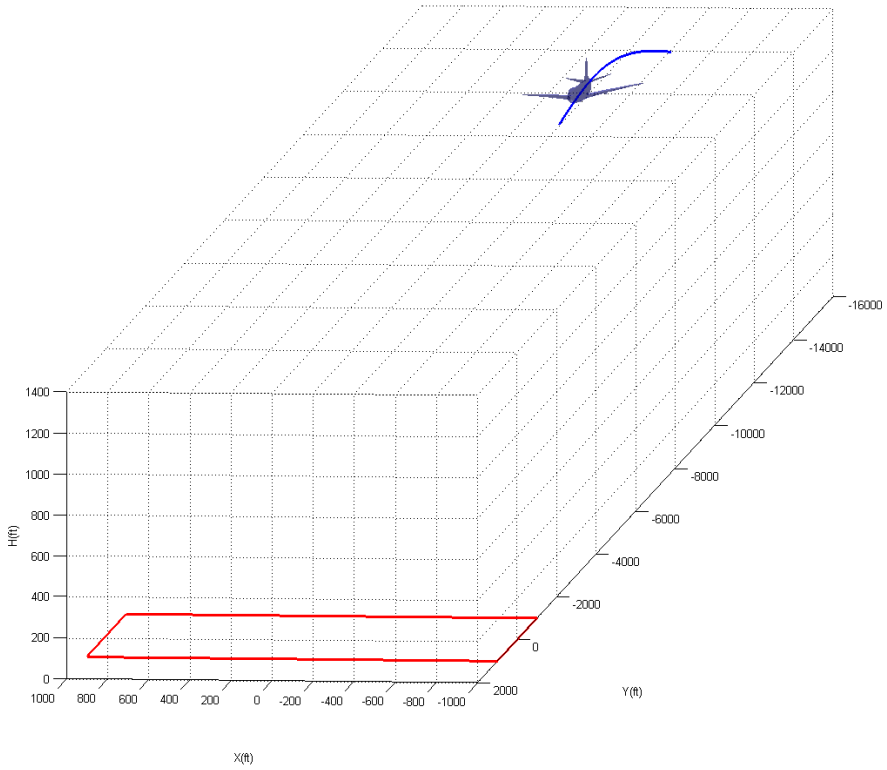

Fig. 1 Landing phase representation

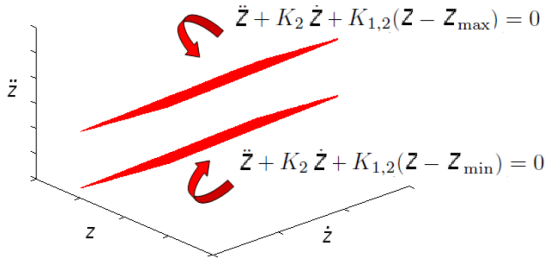

Fig. 2 Representation of the method for relative degree 2 case

Assume the existence of $K_1^1, \ldots, K_{r_1}^1 > 0$ and $K_1^2, \ldots, K_{r_2}^2 > 0$ such that the initial conditions (state) $x(0)$ satisfies:
$\forall k \in [1,2], \forall j \in [0, r_k - 1]$,

$$K^k_{1,j} z_{k,\min} \leq \sum_{i=0}^{j} K^k_{i+1,j} L^i_f \sigma_k(x(0)) \leq K^k_{1,j} z_{k,\max}$$

then it is possible to find a saturation for the control law u which is state-dependent and such that z_1 (resp.z_2) will stay in $[z_{1,\min}, z_{1,\max}]$ (resp.$[z_{2,\min}, z_{2,\max}]$).

Proof: See Annex.

2.5 Output constraint method applied to the case of a landing aircraft

In this application case, it is assumed that a reference image has been taken along the reference trajectory. To this reference image, taken at reference time t_i, is associated the "error position" $\bar{\delta}_x = x(t) - x_c(t_i), \bar{\delta}_y = y(t) - y_c(t_i), \bar{\delta}_z = z(t) - z_c(t_i)$, at every instant. Based on this piece of information, and using the above expression for the homography matrix, given the direction $[v_1^*; v_2^*; v_3^*]$ of the ground point in the reference image, it is possible to compute the linearized homography matrix and the current image frame coordinates of the ground point ([12]), namely:

$$\begin{cases} v_1 := v_1^* + v_2^* \psi - v_3^* \theta \\ v_2 := v_1^* \left(-\psi + \frac{\bar{\delta}_y \tan(\gamma_c)}{|z_c(t_i)|} \right) + v_2^* + v_3^* \left(\phi - \frac{\bar{\delta}_y}{|z_c(t_i)|} \right) \\ v_3 := v_1^* \left(\theta + \frac{\bar{\delta}_z \tan(\gamma_c)}{|z_c(t_i)|} \right) - v_2^* \phi + v_3^* \left(1 - \frac{\bar{\delta}_z}{|z_c(t_i)|} \right) \end{cases}$$

It can be checked that $\forall t,\ v_1 \neq 0$.
The outputs to be constrained, namely the ground point normalized image coordinates, are given by:

$$w_1 := \frac{v_2}{v_1} \qquad \& \qquad w_2 := \frac{v_3}{v_1}$$

They have to be kept inside $[-1, 1]$ in order to maintain the point inside the camera FoV. Also, the inputs are p and q, so that the relative degrees of the outputs with respect to the inputs are $r_1 = r_2 = 1$.
To be able to apply the main theorem proposed above, it is possible to show that the following matrix needs to be invertible:

$$M_z(x) = \frac{1}{v_1} \begin{bmatrix} v_3^* & v_3^* w_1 \\ -v_2^* & v_1^* + v_3^* w_2 \end{bmatrix}$$

Since we know that $v_1 \neq 0$ and $v_3^* \neq 0$, M_z is known to be invertible iff:

$$v_1^* + v_2^* w_1 + v_3^* w_2 \neq 0$$

thus, the outputs can be enforced to remain in their allowed range iff they abide by their constraints at $t = 0$ and the following geometrical condition is satisfied:

$$\mathbf{v}^{*T} \begin{bmatrix} 1 \\ w_1 \\ w_2 \end{bmatrix} \neq 0 \tag{7}$$

This condition has nicely a simple geometrical interpretation: it is the scalar product of two vectors, namely the vector v^* -the target point direction in the reference image- and the vector $[1, w_1, w_2]^T$ -the target point direction in the current image. The condition thus consists in these vectors not being perpendicular to one another. Indeed, would they be perpendicular, the image coordinates of the point would no more be controllable from the two controls: when moving in one or the other direction, it would not change one of the point image coordinates, so that it would not be possible to satisfy the constraint. Note that this condition cannot happen with a 45 ° field of view videocamera if the ground point vector v^* is not chosen on the edge of the image and if the constraint is satisfied at the initial time and later on from the output constraint method. Indeed, the two vectors cannot be perpendicular since they are both inside the camera field of view.

We need to compute f_w such that $\dot{w}_1$ and $\dot{w}_2$ are of the form :

$$\begin{bmatrix} \dot{w}_1 \\ \dot{w}_2 \end{bmatrix} = f_w(x) + M_z(x) \begin{bmatrix} p \\ q \end{bmatrix}$$

Because $r_1 = r_2 = 1$ and because the constrained variables are maintained in $[-1, 1]$, we conclude that our inputs saturations for $k \in [1, 2]$ are limited by the following terms:

$$\begin{aligned} h_1^k(x) &= -K_1^k(w_k + 1) - e_k^T f_w(x) \\ h_2^k(x) &= -K_1^k(w_k - 1) - e_k^T f_w(x) \end{aligned}$$

With our basic control law $[p, q]$, the final control law $[p^{sat}, q^{sat}]$ is given by:

$$\begin{bmatrix} p^{sat} \\ q^{sat} \end{bmatrix} = [M_z(x)]^{-1} \begin{bmatrix} Sat_{h_1^1(x)}^{h_2^1(x)} \left(\frac{v_3^* p + v_3^* w_1 q}{v_1} \right) \\ Sat_{h_1^2(x)}^{h_2^2(x)} \left(\frac{-v_2^* p + (v_1^* + v_3^* w_2) q}{v_1} \right) \end{bmatrix}$$

3 Simulation results

The simulation results are now presented. The UAV trajectory is represented on Fig. 3 and 4, from a longitudinal viewpoint. The green lines show the constraint effect: the trajectory is slightly modified, in order to maintain the ground object inside the FoV.

In a similar way, Fig.5 depicts the lateral viewpoint trajectory. Again, the trajectory is modified by the output constraint.

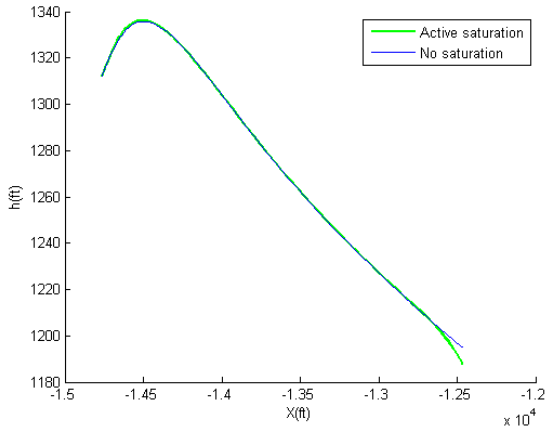

Fig. 3 View of the longitudinal trajectory

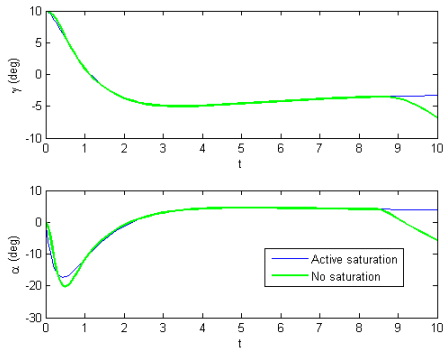

Fig. 4 Longitudinal trajectory angles

Fig. 7 shows the constraint variables evolution (w_1, w_2). The variable keeps increasing, since the ground point gets closer to the edge of the current image. Without the constraint method, the variable would increase and get outside its allowed range, while the proposed method ensures that it is maintained in its limits. In a further study, we shall consider the case of a sequence of reference images.

Fig. 8 finally represents the control variables variation, with green lines depicting the output constrained case; the method has a visible effect on the controls, and this effect enforces the desired constraint.

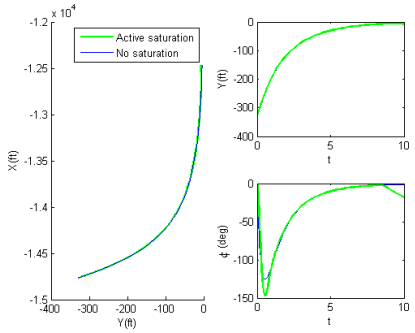

Fig. 5 View of the lateral trajectory

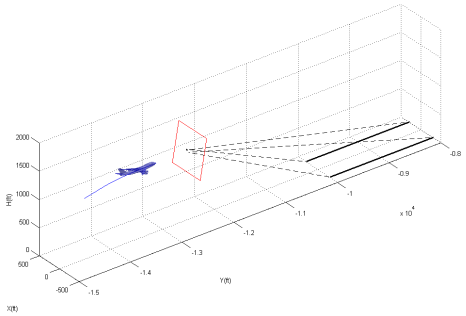

Fig. 6 Trajectory view with current image

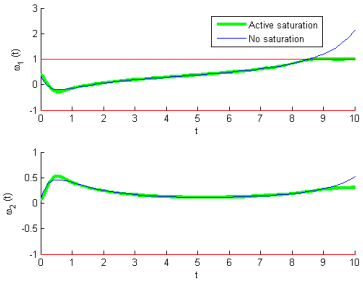

Fig. 7 Evolution of $w_1(t)$, $w_2(t)$ with their desired limits

4 Conclusion

In this paper, a control law able to have a UAV automatically landing while maintaing a ground target point inside a videocamera field of view has been proposed.

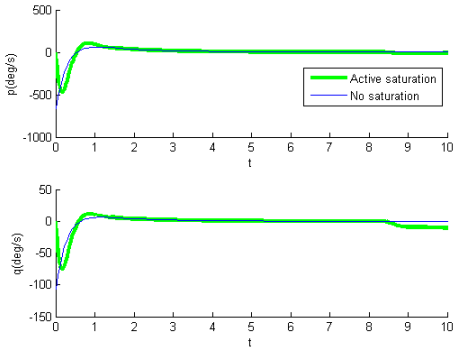

Fig. 8 Evolution of the controls

To this end, a recently developed output constraint method was used, and its application to this case was presented. One must notice the importance of this result: indeed, most visual servoing studies make the assumption that the target does not exit outside the camera field of view, while this requirement is forced in our control scheme. This method thus opens new prospectives in the visual servoing field. Future directions include the use of a sequence of reference images, and the application of this method to other classes of vehicles.

Annex: output constraint method principle

We first recall the principle of the method for the case where one output z is to be restricted inside a given interval $[z_{\min}, z_{\max}]$, and where the system is controlled by a single input u.
We consider the class of nonlinear systems described by:

$$\begin{cases} \dot{x} = f(x) + g(x)u \\ z = \sigma_1(x) + \sigma_2(x)u \end{cases} \tag{8}$$

with f, g, σ_1, σ_2 in $\mathscr{C}^\infty$, $x \in \mathscr{R}^n$ fully measured, the control u and the constrained output z belonging to $\mathscr{R}$.
The proposed method can be summarized as:

1. the relative degree 'r' of the constrained output with respect to the input has to be computed. It is the number of times one needs to derivate the output before seeing the input appearing in the 'r'th order derivative. Let: $r = d_u^{rel} z$.
2. the following remarks can be made:
   - if $d_u^{rel} z = 0$ (i.e $\sigma_2 \neq 0$), then the output depends on the input and limiting the input u and the output z are strictly equivalent:

$$z \in [z_{\min}, z_{\max}] \Leftrightarrow u \in \left[\frac{z_{\min} - \sigma_1}{\sigma_2}, \frac{z_{\max} - \sigma_1}{\sigma_2} \right]$$

- if $d_u^{rel} z = 1$, we note that:

$$\dot{z} = L_f \sigma_1 + (L_g \sigma_1) u \quad \textit{where } L_g \sigma_1 \neq 0$$

In this situation, one may want to use a 'switching' control scheme u which verifies :

$$\begin{cases} (L_g \sigma_1) u \leq -L_f \sigma_1 & \textit{when } z = z_{\max} \\ (L_g \sigma_1) u \geq -L_f \sigma_1 & \textit{when } z = z_{\min} \end{cases}$$

This scheme is not, however, desirable:
– it consists in a 'switching law' and not in a saturation on u
– there is no obvious way to extend this design to a higher relative degree $d_u^{rel} z$.

3. instead, for the relative degree 1 case, given any constant $K > 0$, one can apply the following constraint :

$$\dot{z} \in [-K(z - z_{\min}), -K(z - z_{\max})] \tag{9}$$

As a result, z will remain inside $[z_{\min}, z_{\max}]$ provided its initial value is already. Note that this is the same as using the following saturation :

$$(L_g \sigma_1) u \in [-L_f \sigma_1 - K(z - z_{\min}), -L_f \sigma_1 - K(z - z_{\max})] \tag{10}$$

thus the problem is cast as an input constraint and, most interestingly, can be applied iteratively when $d_u^{rel} z > 1$.
Let us consider the case where $d_u^{rel} z = 2$. Let us use two times a condition of the form (10). Given $K_1 > 0$, one would like to apply:

$$\dot{z} \in [-K_1(z - z_{\min}), -K_1(z - z_{\max})] \tag{11}$$

This is however not possible to apply directly this constraint since $d_u^{rel} z = 2$ so that $\dot{z}$ does not contain u. Let us write

$$\begin{cases} \dot{z}_{\min} := -K_1(z - z_{\min}) \\ \dot{z}_{\max} := -K_1(z - z_{\max}) \end{cases}$$

For $K_2 > 0$, let us consider enforcing

$$\ddot{z} \in [-K_2(\dot{z} - \dot{z}_{\min}), -K_2(\dot{z} - \dot{z}_{\max})] \tag{12}$$

Written in this form, the constraint is equivalent to a constraint on the control u since $d_u^{rel} z = 2$. As a conclusion, keeping the trajectory $t \longmapsto (z(t), \dot{z}(t), \ddot{z}(t))$ between two hyperplanes of the space $(z, \dot{z}, \ddot{z})$ (see Fig. 2) is enough to ensure the desired constraint.

Annex: Theorem Proof

The relative degrees r_1 and r_2 definitions provide:

$$\begin{bmatrix} z_1^{(r_1)} \\ z_2^{(r_2)} \end{bmatrix} = \begin{bmatrix} L_f^{r_1}\sigma_1(x) \\ L_f^{r_2}\sigma_2(x) \end{bmatrix} + M_z(x)\begin{bmatrix} u_1 \\ u_2 \end{bmatrix}$$

Let:

$$\begin{bmatrix} \Gamma_1 \\ \Gamma_2 \end{bmatrix} := M_z(x)\begin{bmatrix} u_1 \\ u_2 \end{bmatrix}$$

the constrained outputs are decoupled with respect to the inputs Γ_1, Γ_2 so that Γ_1 (resp. Γ_2) may be used to maintain z_1 (resp.z_2) inside its range.
Theorem 1 from [18] applied for $k \in [1,2]$ ensures that if the input Γ_k is maintained inside $[h_1^k(x), h_2^k(x)]$ with:

$$\begin{aligned} h_1^k(x) &= K_{1,r_k}^k z_{\min}^k - \textstyle\sum_{i=0}^{r_k} K_{i+1,r_k}^k L_f^i \sigma_k(x) \\ h_2^k(x) &= K_{1,r_k}^k z_{\max}^k - \textstyle\sum_{i=0}^{r_k} K_{i+1,r_k}^k L_f^i \sigma_k(x) \end{aligned}$$

then the output z_k will be maintained in $[z_{k,\min}, z_{k,\max}]$ as long as the initial state is such that $\forall j \in [0, r_k - 1]$:

$$K_{1,j}^k z_{k,\min} \leq \textstyle\sum_{i=0}^{j} K_{i+1,j}^k L_f^i \sigma_k(x(0)) \leq K_{1,j}^k z_{k,\max}$$

To conclude the proof, we go back to the inputs u_1 and u_2. Let u_1^{sat} and u_2^{sat} be the corresponding saturated outputs. Indeed, since M_z is invertible, saturating Γ_k by $Sat_{h_1^k(x)}^{h_2^k(x)}$ leads to :

$$\begin{aligned} \begin{bmatrix} u_1^{sat} \\ u_2^{sat} \end{bmatrix} &= [M_z(x)]^{-1} \begin{bmatrix} Sat_{h_1^1(x)}^{h_2^1(x)}(\Gamma_1(x)) \\ Sat_{h_1^2(x)}^{h_2^2(x)}(\Gamma_2(x)) \end{bmatrix} \\ &= [M_z(x)]^{-1} \begin{bmatrix} Sat_{h_1^1(x)}^{h_2^1(x)}\left(e_1^T M_z(x)\begin{matrix} u_1 \\ u_2 \end{matrix}\right) \\ Sat_{h_1^2(x)}^{h_2^2(x)}\left(e_2^T M_z(x)\begin{matrix} u_1 \\ u_2 \end{matrix}\right) \end{bmatrix} \end{aligned}$$

References

1. J. R. Azinheira and P. Rives and J. R. H. Carvalho and G. F. Silveira and E. C. de Paiva and S. S. Bueno, *Visual Servo Control for the Hovering of an Outdoor Robotic Airship*, IEEE International Conference on Robotics and Automation, 2002
2. J. R. Azinheira and P. Rives, *Image-Based Visual Servoing for Vanishing Features and Ground Lines Tracking: Application to UAV Automatic Landing*, International Journal of Optomecha-

tronics, vol.2(3), pp. 275-295, 2008
3. F. Le Bras and T. Hamel and C. Barat and R. Mahony, *Nonlinear Image-Based Visual Servo controller for automatic landing guidance of a fixed-wing Aircraft*, Proc. of the European Control Conference, pp. 1836-1841, 2009
4. G. Lopez-Nicolas and S. Bhattacharya and J.J. Guerrero and C. Sagues and S. Hutchinson , *Switched Homography-Based Visual Control of Differential Drive Vehicles with Field-of-View Constraints*, IEEE International Conference on Robotics and Automation, 2007
5. R. Cunha and C. Silvestre and J.P. Hespanha and A. P. Aguiar, *Vision-based control for rigid body stabilization*, Automatica, pp. 1020-1027, 2011
6. Z. Zhang and A. R. Hanson, *3D Reconstruction Based on Homography Mapping*, In ARPA Image Understanding Workshop, pp. 0249-6399, 1996
7. S. Benhimane and E. Malis and P. Rives J. R. Azinheira, *Vision-based Control for Car Platooning using Homography Decomposition*, IEEE Conference on Robotics and Automation, pp. 2161-2166, 2005
8. J.J Guerrero and R. Martinez-Cantin and C. Sagués , *Visual map-less navigation based on homographies*, Journal of Robotic Systems, pp. 569-581, 2005
9. M. Vargas and E. Malis, *Visual servoing based on an analytical homography decomposition*, IEEE Conference on Decision and Control and European Control Conference, pp. 5379-5384 , 2005
10. E. Malis and M. Vargas , *Deeper understanding of the homography decomposition for vision-based control*, INRIA technical report, 2007
11. N. Simond and C. Laurgeau, *Vehicle Trajectory from an Uncalibrated Stereo-Rig with Super-Homography*, IEEE International Conference on Robotics and Systems , pp. 4768-4773, 2006
12. S. Benhimane and E. Malis , *Homography-based 2D Visual Tracking and Servoing*, International Journal of Robotic Research, pp. 661-676, 2007
13. D.S. Bernstein and A. N. Michel, *A chronological bibliography on saturating actuators*, International Journal of Robust and Nonlinear Control, vol.5, pp. 375-380, 1995.
14. T. Hu, *Nonlinear feedback laws for practical stabilization of systems with input and state constraints*, Proc. of the 47th Conference on Decision and Control, Cancun, Mexico, pp. 3481-3486, 2008.
15. M.C. Turner and I. Postlethwaite, *Output violation compensation for systems with output constraints*, IEEE Transactions on Automatic Control, vol.47(9), pp. 1540-1546, 2002.
16. E.G. Gilbert and K.T. Tan, *Linear systems with state and control constraints: the theory and application of maximal output admissible sets*, IEEE Transactions on Automatic Control, vol.36(9), pp. 1008-1020, 1991.
17. O.J. Rojas and G.C. Goodwin, *A simple anti-windup strategy for state constrained linear control*, Proc. of the 15th IFAC World Congress, Barcelona, Spain, 2002.
18. L. Burlion, *A new Saturation function to convert an output constraint into an input constraint*, 20th Mediterranean Conference on Control and Automation, pp. 1217-1222, 2012.
19. F. Allgöwer and A.Z. Zheng, *Nonlinear model predictive control : assessment and future directions for research*, Progress in Systems and control Series, Birkhäuser Verlag, Basel, 2000.
20. E. Gilbert and I. Kolmanovsky, *Nonlinear tracking control in the presence of state and control constraints : a generalized reference governor*, Automatica, vol.38, pp. 2063-2073, 2002.
21. P. Mhaskar, N.H. El-Farra and P.D. Christofides, *Stabilization of nonlinear systems with state and control constraints using Lyapunov-based predictive control*, Syst. & Contr. Lett., vol. 55, pp. 650-659, 2006.
22. K. Graichen and M. Zeitz, *Feedforward control design for finite-time transition problems of nonlinear systems with input and output constraints*, IEEE Transactions on Automatic Control, vol.53(5), pp. 1273-1278, 2008.
23. K.B. Ngo, R. Mahony and J. Zhong-Ping, *Integrator backstepping using barrier functions for systems with multiple state constraints*, Proc. of the 44th Conference on Decision and Control, Seville, Spain, pp. 8306-8312, 2005.
24. K.P. Tee, S.S. Ge and E.H. Tay, *Barrier Lyapunov functions for the control of output-constrained nonlinear systems*, Automatica, vol.45(4), pp. 918-927, 2009.

25. J.R. Cloutier and J.C. Cockburn, *The state-dependent nonlinear regulator with state constraints*, Proc. of the American Control Conference, Arlington, Texas, pp. 390-395, 2001.
26. M. Bürger and M. Guay, *Robust Constraint Satisfaction for Continuous-time Nonlinear Systems in Strict Feedback Form*, IEEE Transactions on Automatic Control, vol.55(11), pp. 2597-2601, 2010.
27. E. Malis and P. Rives , *Robustness of Image-Based Visual Servoing with Respect to Depth Distribution Errors*, IEEE International Conference on Robotics and Automation, pp. 1056-1061, 2003.